Electronic Supplementary Material (ESI) for RSC Advances.
This journal is © The Royal Society of Chemistry 2016

Synthesis, characterization, crystal structure of RNA targeted L- and D-phenylalanine-(1, 10-phen)-copper(II) conjugate complexes; Comparative *in vitro* RNA binding profile of enantiomers and their biological evaluation by morphological studies and antibacterial activity

Surbhi Sharma,[a] Loic Toupet[b], Musheer Ahmad[c] and **Farukh Arjmand[a,*]**

[a]*Department of Chemistry, Aligarh Muslim University, Aligarh 202002, India.*
[b]*Institut de Physique de Rennes, UMR 625, Université de Rennes 1, Campus de Beaulieu Bat. 11 A, 263 av. Général Leclerc, 35042 Rennes Cedex, France.*
[c]*Department of Applied Chemistry, Aligarh Muslim University, Aligarh 202002, India.*
*E−mail: farukh_arjmand@yahoo.co.in. *Corresponding author. Tel.: +91 5712703893

Table S1. Selected bond lengths for complex **1a**, $C_{21}H_{22}CuN_4O_7$

Bond lengths	(Å)
Cu(1)-O(2)	1.941(2)
Cu(1)-N(3)	1.993(3)
Cu(1)-N(2)	2.004(3)
Cu(1)-N(1)	2.029(3)
Cu(1)-O(1)	2.199(3)
O(2)-C(13)	1.281(4)
O(3)-C(13)	1.232(4)
O(4)-N(4)	1.240(5)
O(5)-N(4)	1.227(5)
O(6)-N(4)	1.230(5)
N(1)-C(1)	1.326(4)
N(1)-C(12)	1.354(4)
N(2)-C(10)	1.323(5)
N(2)-C(11)	1.358(4)
N(3)-C(14)	1.490(4)

Table S2. Selected bond angles for complex **1a**, $C_{21}H_{22}CuN_4O_7$

Bond Angle	[deg]
O(2)-Cu(1)-N(3)	84.59(10)
O(2)-Cu(1)-N(2)	92.24(10)
N(3)-Cu(1)-N(2)	168.26(11)
O(2)-Cu(1)-N(1)	163.45(10)
N(3)-Cu(1)-N(1)	97.49(11)
N(2)-Cu(1)-N(1)	82.41(11)
O(2)-Cu(1)-O(1)	105.60(11)
N(3)-Cu(1)-O(1)	98.61(11)
N(2)-Cu(1)-O(1)	93.13(11)
N(1)-Cu(1)-O(1)	90.37(11)
C(13)-O(2)-Cu(1)	116.3(2)
C(1)-N(1)-C(12)	118.3(3)

C(1)-N(1)-Cu(1)	130.2(2)
C(12)-N(1)-Cu(1)	111.3(2)
C(10)-N(2)-Cu(1)	128.7(2)
C(11)-N(2)-Cu(1)	112.4(2)
C(14)-N(3)-Cu(1)	110.41(19)

Table S3. Selected bond lengths for complex **1b**, $C_{21}H_{22}CuN_4O_7$

Bond lengths	**(Å)**
Cu(1)-O(1)	1.941(2)
Cu(1)-N(1)	1.985(3)
Cu(1)-N(2)	2.024(3)
Cu(1)-N(3)	2.001(3)
Cu(1)-O(3)	2.191(3)
O(1)-C(1)	1.283(4)
O(2)-C(1)	1.230(4)
O(4)-N(4)	1.245(4)
O(5)-N(4)	1.234(5)
O(6)-N(4)	1.243(5)
N(2)-C(10)	1.327(4)
N(3)-C(20)	1.360(4)
N(1)-C(2)	1.484(4)

Table S4. Selected bond angles for complex **1b**, $C_{21}H_{22}CuN_4O_7$

Bond Angle	**[deg]**
O(1)-Cu(1)-N(1)	84.56(10)
O(3)-Cu(1)-N(3)	92.71(11)
N(1)-Cu(1)-N(3)	168.23(11)
O(1)-Cu(1)-N(2)	163.64(9)
N(1)-Cu(1)-N(2)	97.45(11)
N(3)-Cu(1)-N(2)	82.51(11)
O(1)-Cu(1)-O(3)	105.96(11)
N(1)-Cu(1)-O(3)	99.06(12)
N(2)-Cu(1)-O(3)	89.81(11)
N(3)-Cu(1)-O(3)	92.71(11)
C(1)-O(1)-Cu(1)	116.09(19)

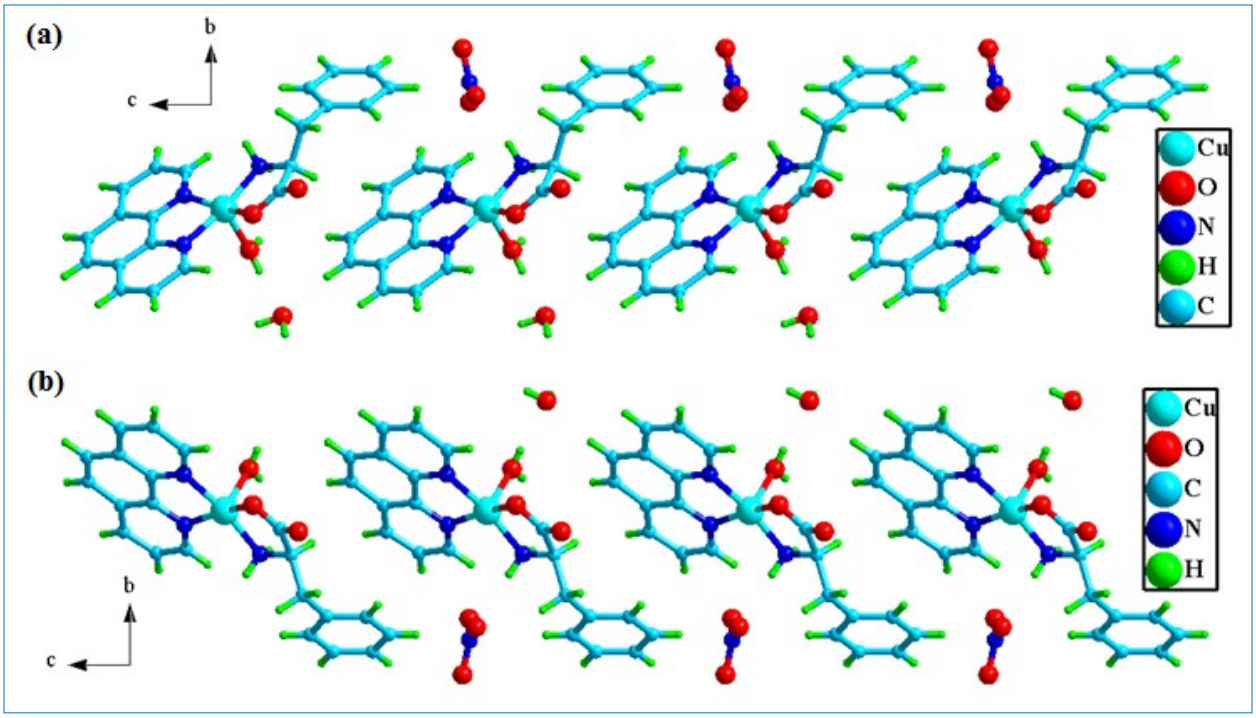

Fig. S1 Packing diagram of **(a)** complex **1a** and **(b)** complex **b.**

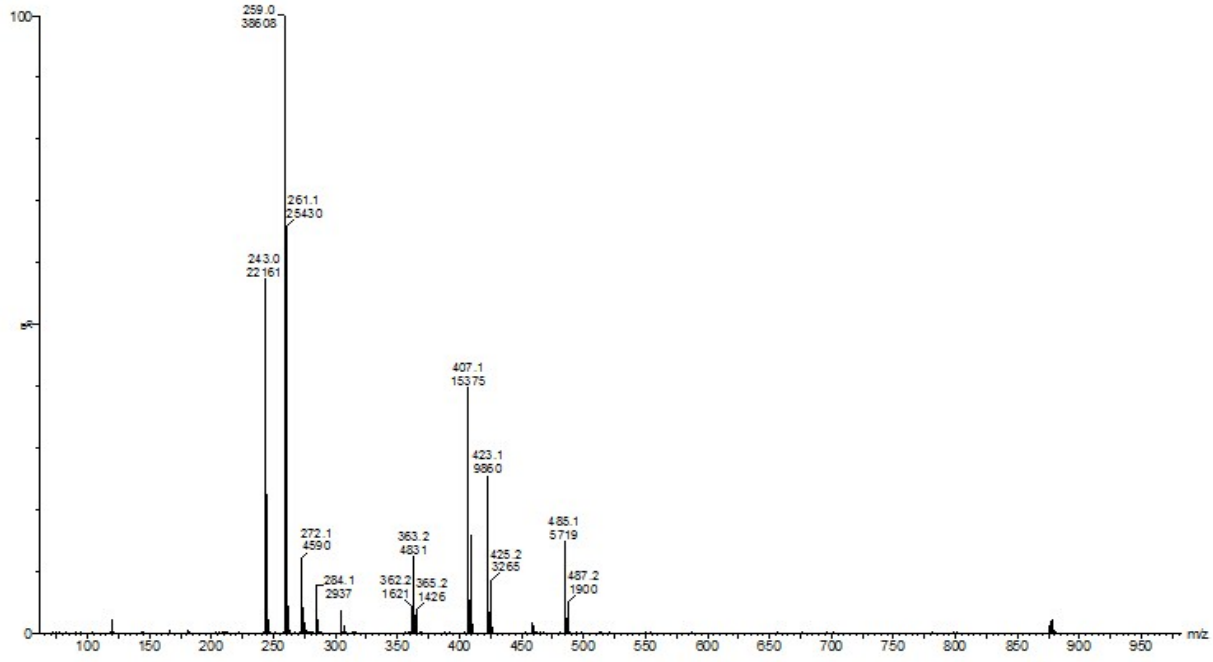

Fig. S2 ESI-MS spectrum of complex **1a**

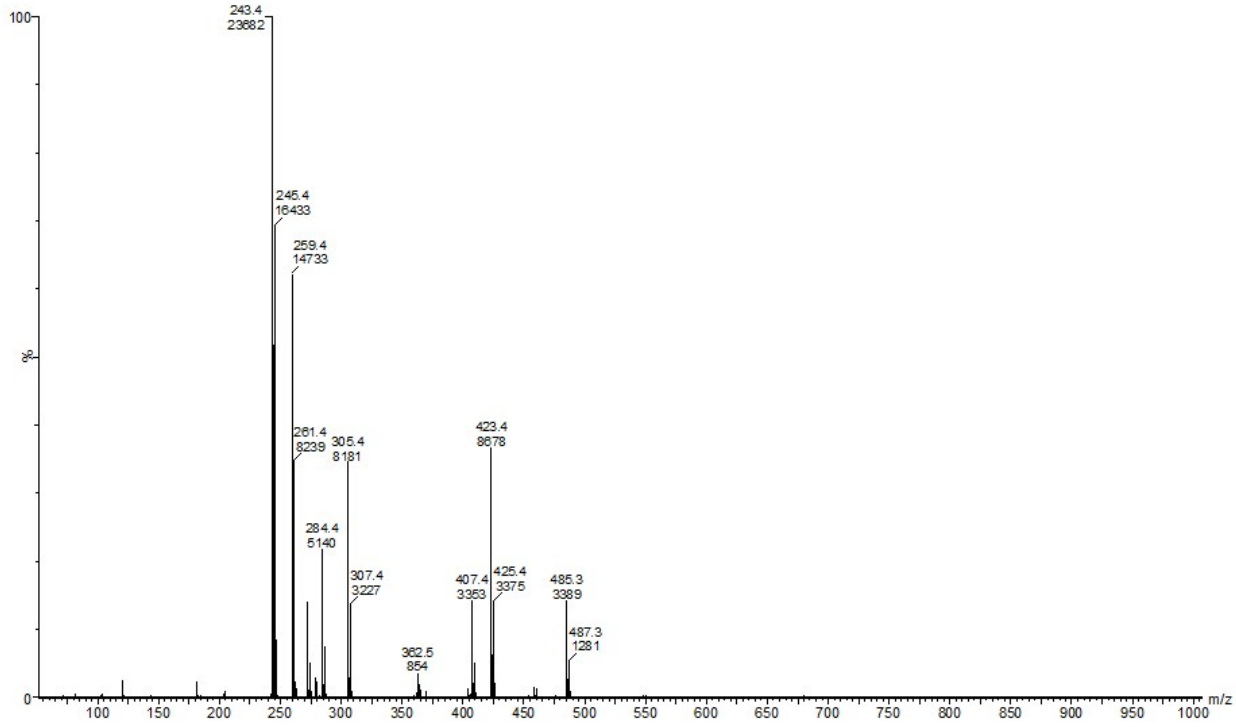

Fig. S3 ESI-MS spectrum of complex **b**

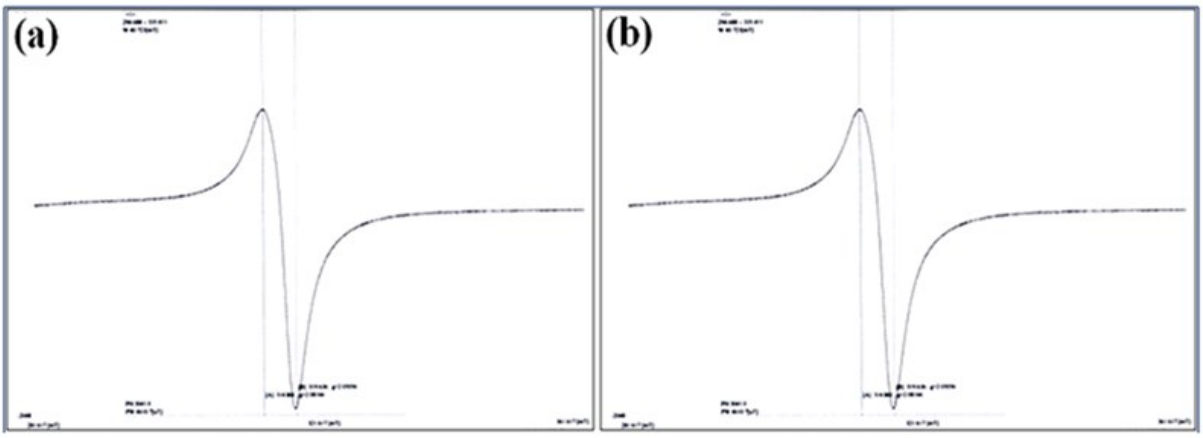

Fig. S4 X–band EPR spectrum of complex (a) **1a and** (b) **b** at RT.

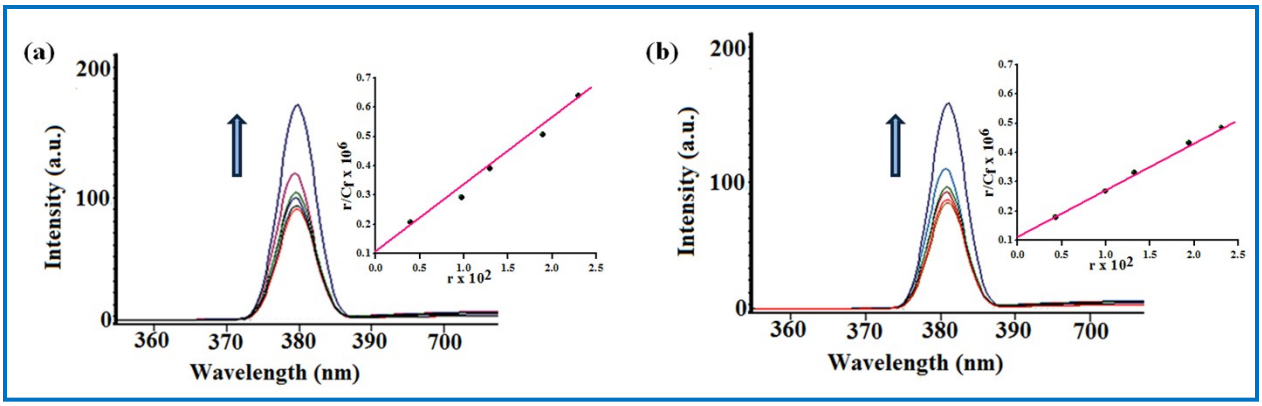

Fig. S5 Emission spectra of complex **1a** and **b** in Tris–HCl buffer at pH 7.2 upon addition of yeast tRNA. [RNA] = 0.00–4.00 x 10^{-5} M, [Complex] = 1.67 x 10^{-4} M. Arrows show change in intensity with increasing concentration of RNA.

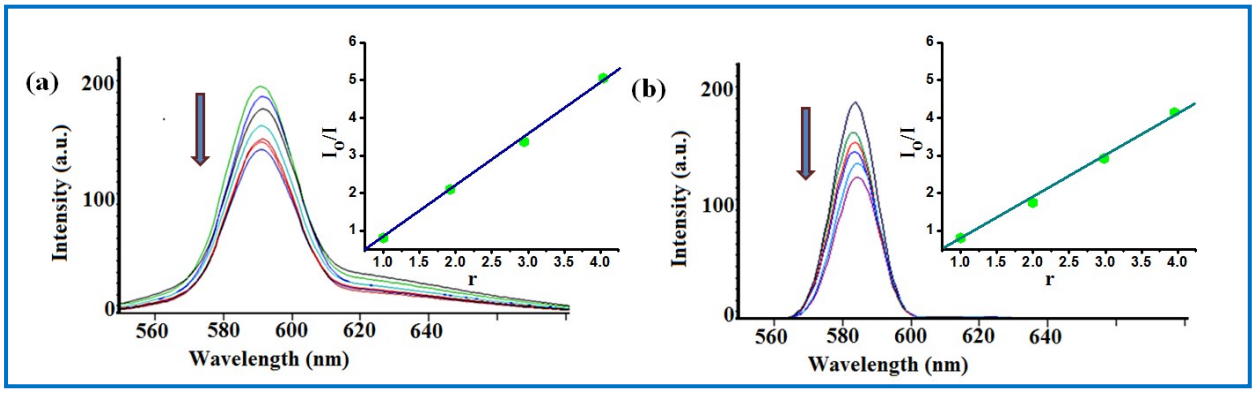

Fig. S6 Emission spectra of EB–yeast tRNA in the absence and presence of complex **1a** and **b** in Tris–HCl buffer at pH 7.2. [Complex] = [EB] = [RNA] = 1.11 x 10^{-4} M. Arrow shows change in intensity with increasing concentration of complex **1a** and **b**.

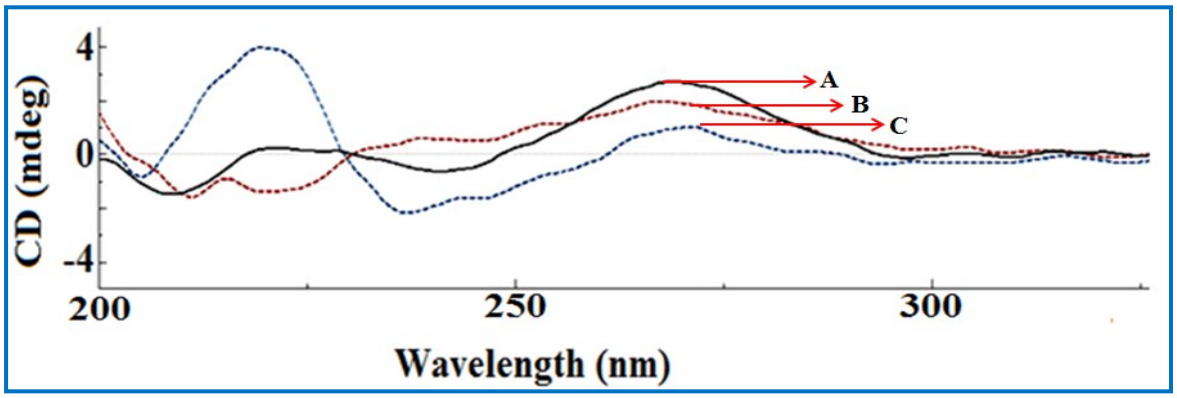

Fig. S7 CD spectra of **(A)** t-RNA alone, **(B)** t-RNA in presence of complex **1a**, **(C)** t-RNA in presence of complex **b** in Tris-HCl buffer at 25℃. [Complex] = 1 x 10^{-4} M and [t-RNA] = 1 x 10^{-4} M.

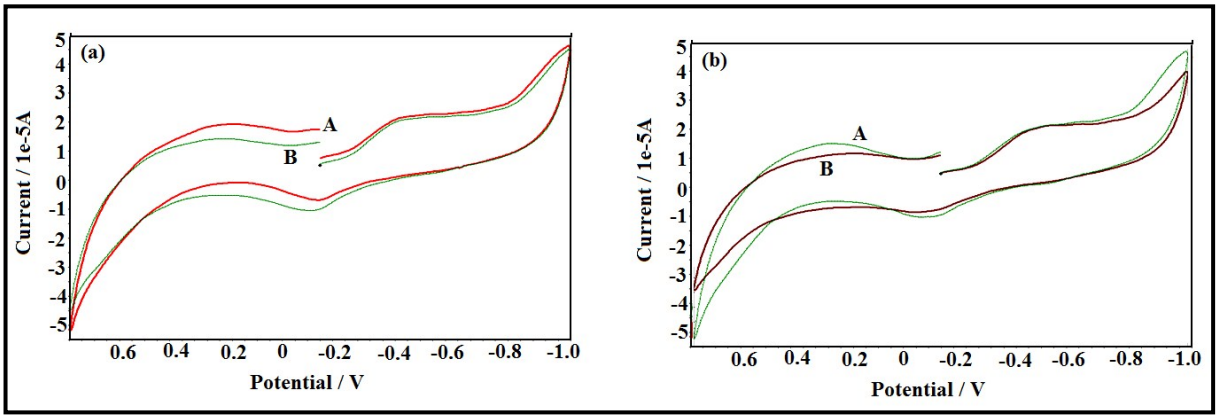

Fig. S8 (a) Cyclic voltammogram (5:95 DMSO/H2O, 25℃) of (**A**) unbound complex **1a** and (**B**) complex **1a** in presence of t-RNA. **(b)** Cyclic voltammogram (5:95 DMSO/H2O, 25℃) of (**A**) unbound complex **1b** and (**B**) complex **1b** in presence of t-RNA at a scan rate of 0.2 Vs^{-1}. [Complex] = 1 x 10^{-3} and [t-RNA] = 4 x 10^{-3}.